

Probing the Nature of High- z Short GRB 090426 with Its Early Optical and X-ray Afterglows

Li-ping Xin^{1*}, En-wei Liang^{2†}, Jian-yan Wei¹, Bing Zhang³, Hou-jun Lv², Wei-kang Zheng⁴, Yuji Urata⁵, Myungshin Im⁶, Jing Wang¹, Yu-lei Qiu¹, Jin-song Deng¹, Kui-yun Huang⁵, Jing-yao Hu¹, Yiseul Jeon⁶, Hua-li Li¹ and Xu-hui Han¹

¹ National Astronomical Observatories, Chinese Academy of Sciences, Beijing 100012, China.

² Department of Physics, Guangxi University, Guangxi 530004, China.

³ Department of Physics and Astronomy, University of Nevada, Las Vegas, Nv 89154, USA.

⁴ Department of Physics, University of Michigan, Ann Arbor, MI 48109, USA.

⁵ Institute of Astronomy, National Central University, Chung-Li 32054, Taiwan, Republic of China.

⁶ Center for the Exploration of the Origin of the Universe, Department of Physics & Astronomy, FPRD, Seoul National University, Shillim-dong, San 56-1, Kwanak-gu, Seoul, Korea.

Accepted Received: Revision 1

ABSTRACT

Swift GRB 090426 is a short duration burst ($T_{90} \sim 0.33$ seconds in the burst frame at $z = 2.609$) with analogous properties on its host galaxy and spectrum-energy correlation to typical long duration GRBs from collapses of massive stars (Type II GRBs). We present its early optical observations with 0.8-m TNT telescope at Xinglong observatory and 1-m telescope at Mt. Lemmon Optical Astronomy Observatory LOAO in Arizona. Our well-sampled optical afterglow lightcurve covered from ~ 90 seconds to $\sim 10^4$ seconds post the GRB trigger shows two energy injection phases ended at ~ 230 seconds and ~ 7100 seconds, respectively. The decay slopes post the injection phases are consistent with each other ($\alpha \simeq 1.22$). The X-ray afterglow lightcurve seems to trace the optical one, although the second energy injection phase was missed due to the orbit constrain of Swift satellite. The spectral index of the X-rays is ~ 1.0 without temporal evolution. The X-ray emission is consistent with the forward shock models. Both the X-ray and optical emission would be in the same spectral regime above the cooling frequency (ν_c). The fact that the ν_c is below the optical bands since a very early epoch constrains the burst in a medium environment similar to typical Type II GRBs, hence suggests the death of a massive star as a possible progenitor of this burst.

Key words: gamma rays: bursts (individual: GRB 090426)—gamma rays: observations.

1 INTRODUCTION

Cosmic gamma-ray bursts (GRBs) are classified into two groups with the observed burst duration of $T_{90} \sim 2$ seconds based on CGRO/BATSE observations (Kouveliotou et al. 1993). Properties of the afterglows and host galaxy of long GRBs, especially detections of most long GRB-supernova connection, well suggest that they are likely related to deaths of massive stars, and the ‘‘collapsar’’ model has been widely

recognized as the standard scenario for long GRBs (Woosley 1993; Paczyński 1998; Zhang & Mészáros 2004; Piran 2004; Woosley & Bloom 2006). Observations for some short GRBs with *Swift* and other instruments (Gehrels et al. 2005; Villaseñor et al. 2005; Fox et al. 2005; Berger et al. 2005; McGlynn et al. 2008) show that they are associated with nearby early-type galaxies with little star formation and without detection of associated supernova (Zhang et al. 2007a; Nakar 2007), favoring the idea that short GRBs are from mergers of two compact stellar objects (Eichler et al. 1989; Narayan et al. 1992).

* email: xlp@bao.ac.cn

† email: lew@gxu.edu.cn

Swift observations reveal that the long-short GRB classification scheme is found not always to match the physical classification scheme of Type II (collapses of massive stars) vs. Type I (mergers of compact stars) (Zhang et al. 2006; Zhang et al. 2007a; Zhang et al. 2009; Lv et al. 2010). Some convincing Type I GRBs have long, soft “extended emission” (Barthelmy et al. 2005; Norris et al. 2006; Lin et al. 2008; Zhang et al. 2009; Perley et al. 2009), making their T_{90} essentially long. Non-detection of associated supernovae for nearby long GRBs 060614 and 060505 (Gehrels et al. 2006; Gal-Yam et al. 2006; Fynbo et al. 2006) disfavors the Type II origin for these long GRBs. Observations of intrinsically short duration of high- z GRBs 080913 ($z = 6.7$; Greiner et al. 2009a) and 090423 ($z = 8.3$; Tanvir et al. 2009; Salvaterra et al. 2009) show that these “short” GRBs are most likely from collapsars (Zhang et al. 2009; Lin et al. 2009; Levesque et al. 2010; Belczynski et al. 2010). Zhang et al. (2009) and Virgili et al. (2009) suggest that some short duration GRBs are out of Type II origin. Based on the observed gamma-ray energy and peak energy of the νf_ν spectrum of prompt gamma-rays, Lv et al. (2010) proposed a new classification scheme that may can better match the physically-motivated Type II/I classification scheme with a parameter $\varepsilon \equiv E_{\text{iso}}/E_{p,z}^{1.7}$. They show that typical Type II GRBs are of high- ε group.

Another striking case for the conventional long-short GRB classification scheme is GRB 090426. Its observed T_{90} in the BAT band is only 1.2 ± 0.3 second (Sato et al. 2009), corresponding to a rest frame duration of 0.33 at redshift $z = 2.609$ (Levesque et al. 2010). Phenomenologically, it is unambiguously within the range of classical short-type GRBs in both observer and rest-frames. However, both the host galaxy and spectrum-energy properties suggest that it is a Type II GRB, i.e., from core collapse of a massive star (Levesque et al. 2010; Antonelli et al. 2009). With the new classification method proposed by Lv et al. (2010), this event is also well classified into the high- ε group.

Multi-wavelength afterglows are essential for revealing the burst environment, hence can be served as a probe for burst progenitor stars. In this paper, we report our observations of the early optical afterglows for GRB 090426 with TNT telescope at Xinglong and telescope at Mt. Lemmon Optical Astronomy Observatory LOAO in Arizona and explore the nature of this event with the early optical and X-ray afterglows.

Our observations are reported in Section 2, and joint optical and X-ray afterglow data analysis are present in Section 3. Conclusions and discussion are present in Section 4. The notation $f \propto t^{-\alpha} \nu^{-\beta}$ is used throughout the paper.

2 OBSERVATIONS

At 12:48:47 UT, the Swift/Burst Alert Telescope (BAT) triggered and located GRB 090426 (Cummings et al. 2009). Its duration is $T_{90} = 1.28 \pm 0.09$ sec in 15-350 KeV. *Swift* XRT observed the burst at 84.6 sec after the GRB trigger. *Swift* UVOT began observing the burst location at 89 sec after the burst trigger, and reported the optical counterpart with a brightness of about 17.5 mag in the white band. The optical afterglow was confirmed by our team (Xin et al. 2009) and other follow-up teams (e.g. Im et al. 2009). The optical spectrum of its afterglow gives a redshift of 2.609 detected by

Keck telescope (Levesque et al. 2009), which was confirmed by ESO VLT Spectrograph (Thoene et al. 2009). Its time-integrated spectrum is very soft, with an power-law index of 1.93 (Sato et al. 2009), roughly corresponding to an estimate of $E_{\text{peak},o}$ as 45 KeV via an empirical relation between E_p and the powerlaw index in the BAT band (Liang & Zhang 2005; Sakamoto et al. 2009).

2.1 Optical Observation and Data Reduction

We carried out a follow-up observation campaign of *Swift* GRB 090426 with the TNT (0.8-m Tsinghua University-National Astronomical Observatory of China Telescope) at Xinglong Observatory, under the framework of the *EAFON* (Urata et al. 2003; 2005). TNT is equipped with a PI 1300×1340 CCD and filters in the standard Johnson Bessel system. Its field of view is 11.4×11.4 arcmin, yielding 0.5 arcsec of the pixel scale. A custom-designed automation system has been developed for the GRB follow-up observations (Zheng et al. 2008).

The observation of the optical transient (OT) of GRB 090426 (Cummings et al. 2009) was carried out with TNT at 86 seconds post the *Swift*/BAT trigger, which is slightly earlier than the beginning observation of XRT and UVOT on-board *Swift*. A new fading source was detected, with a position being consistent with the UVOT coordinate (Cummings et al. 2009), thus confirmed as the OT of the burst (Xin et al. 2009). The *W* (white), *R* and *V*-band images were obtained in 86–519 seconds, 570 – 1513 seconds, and 1907 – 10748 seconds post the GRB trigger, respectively. The optical afterglow was clearly detected.

The 1-m telescope (Han et al. 2005) is located at Mt. Lemmon Optical Astronomy Observatory LOAO in Arizona operated by the Korea Astronomy Space Science Institute. Observation of GRB 090426 was carried out at about 16.3 hours after the burst ($t \sim 60$ ks) in the *R* filter. The OT was not detected and only an upper limit was obtained.

Data reduction was carried out following standard routine in IRAF¹ package, including bias and flat-field corrections. Dark correction was not performed since the temperature of our CCD was cooled down to -110°C . Point spread function (PSF) photometry was applied via DAOPHOT task in IRAF package to obtain the instrumental magnitudes. During the reduction, some frames were combined in order to increase signal-to-noise ratio (S/N). In the calibration and analysis, the *white* band data was treated as *R* band magnitude (Xin et al. 2010). Absolute calibration was performed using the Sloan Digital Sky Survey (SDSS, Adelman-McCarthy et al. 2008), with conversion of SDSS to Johnson-Cousins system². The data of GRB 090426 obtained by TNT and LOAO are reported in Table. 1.

¹ IRAF is distributed by NOAO, which is operated by AURA, Inc., under cooperative agreement with NSF.

² <http://www.sdss.org/dr6/algorithms/sdssUBVRITransform.html> #Lupton2005

Table 1. Optical Afterglow Photometry Log of GRB 090426. The reference time T_0 is *Swift* BAT burst trigger time. All Data are not corrected for the Galactic extinction of $E_{B-V} = 0.017$ (Schlegel et al.1998). *Merr* means the uncertainty of magnitude.

T-T0(mid) sec	Exposure sec	Mag	Merr	Filter	Telescope
86	20.0	16.44	0.03	W	TNT
109	20.0	16.50	0.03	W	TNT
133	20.0	16.59	0.03	W	TNT
155	20.0	16.66	0.03	W	TNT
178	20.0	16.76	0.03	W	TNT
201	20.0	16.88	0.04	W	TNT
223	20.0	17.01	0.04	W	TNT
246	20.0	17.01	0.04	W	TNT
269	20.0	17.07	0.04	W	TNT
292	20.0	17.09	0.04	W	TNT
314	20.0	17.22	0.04	W	TNT
337	20.0	17.30	0.05	W	TNT
360	20.0	17.31	0.05	W	TNT
382	20.0	17.44	0.05	W	TNT
405	20.0	17.50	0.06	W	TNT
428	20.0	17.56	0.06	W	TNT
451	20.0	17.69	0.06	W	TNT
473	20.0	17.63	0.06	W	TNT
496	20.0	17.80	0.06	W	TNT
519	20.0	17.89	0.06	W	TNT
570	60.0	17.93	0.06	R	TNT
649	60.0	18.12	0.07	R	TNT
728	60.0	18.30	0.07	R	TNT
807	60.0	18.38	0.08	R	TNT
885	60.0	18.46	0.09	R	TNT
964	60.0	18.72	0.08	R	TNT
1042	60.0	18.71	0.08	R	TNT
1121	60.0	18.78	0.11	R	TNT
1199	60.0	18.85	0.11	R	TNT
1278	60.0	19.01	0.11	R	TNT
1356	60.0	19.04	0.12	R	TNT
1435	60.0	19.12	0.12	R	TNT
1513	60.0	19.06	0.12	R	TNT
1907	300×2	19.72	0.12	V	TNT
2542	300×2	20.04	0.12	V	TNT
3178	300×2	20.10	0.12	V	TNT
3813	300×2	20.05	0.12	V	TNT
4448	300×2	20.17	0.12	V	TNT
5084	300×2	20.19	0.14	V	TNT
5878	300×3	20.30	0.14	V	TNT
7048	600×2	20.47	0.16	V	TNT
8282	600×2	20.69	0.17	V	TNT
9515	600×2	20.65	0.17	V	TNT
10748	600×2	20.71	0.18	V	TNT
58591	180×10	>21.67		R	LOAO

2.2 Data Reduction for X-ray Afterglows Observed with Swift/XRT

The *Swift*/XRT lightcurve and spectrum are extracted from the UK Swift Science Data Centre at the University of Leicester (Evans et al. 2009)³. We fit the X-ray spectrum with the *Xspec* package. The time-integrated X-ray spectrum is

³ <http://www.swift.ac.uk/results.shtml>

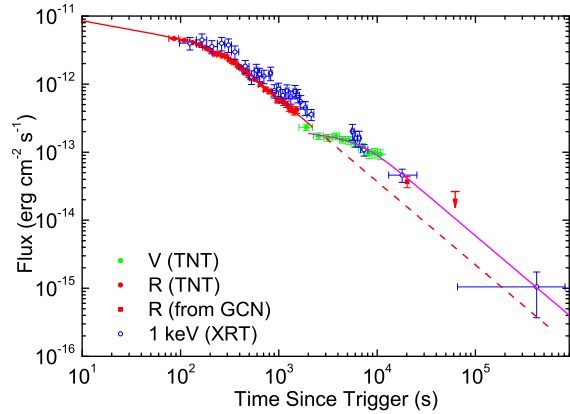


Figure 1. The extinction-corrected optical light curve of GRB 090426 (solid dots) and the best fit with a smooth broken power-law model (solid line) for two epochs before and after 2200 seconds post the GRB trigger. The *R*-band data observed by Rumyantsev et al. (2009) is marked with a square. The XRT lightcurve (open dots) is also shown in comparison.

Table 2. Optical lightcurve fit with a smooth broken power-law model for two epochs.

Interval	F_0^*	t_p (s)	α_1	α_2
86-2200s	3.74 ± 0.32	227 ± 27	0.26 ± 0.07	1.22 ± 0.04
> 2200 s	1.77 ± 0.67	7123 ± 3620	0.19 ± 0.41	~ 1.22

*In units of $\times 10^{-12}$ erg cm^{-2} s^{-1} .

well fit with an absorbed power-law model, yielding a photon power-law index $\Gamma = 2.00 \pm 0.06$ from the PC mode data. No significant host N_H excess over our Galaxy is detected.

3 JOINT ANALYSIS ON THE OPTICAL AND X-RAY AFTERGLOW OBSERVATIONS

3.1 Temporal Analysis

With the X-ray spectral index ($\beta_X = 1.00 \pm 0.06$), we derive the lightcurve at 1 keV from the XRT data. It is shown in Fig. 1. We convert the extinction-corrected magnitudes of the optical afterglows into energy fluxes. Levesque et al. (2010) reported $A_V \sim 0.4$ for the GRB host galaxy, and the extinction by our Galaxy in the burst direction is $A_V = 0.017$ (Schlegel et al.1998). The transformation from A_V to A_R is nearly independent of any known type extinction laws (MW, LMC, SMC). We have $A_R \sim 0.32$. We find that specified νF_ν fluxes in the optical and X-ray bands at the time is almost the same. This indicates a flat νF_ν spectrum from the optical to the X-ray bands, i.e., $\beta_{OX} \sim 1.0$. This is consistent with the observed X-ray spectral index. Therefore, we do not need to calibrate the observed fluxes in the optical bands to a given band. The extinction-corrected optical afterglow lightcurve is shown in Fig. 1.

As shown in Fig. 1, the afterglow lightcurves in the op-

tical and X-ray bands trace with each other, confidently suggesting that they should be in the same spectral regime. At the early epoch $t < 2200$ seconds post the GRB trigger, the optical and X-ray afterglow lightcurves show a smooth shallow-to-normal decaying segment, with small flickerings in the X-ray band. In the time interval $2200 \sim 5500$ seconds, the brightness of the OT kept almost a constant. It then faded again at $t > 5500$ seconds. The OT was also detected by Ruyantsev et al. (2009) at 0.2342 day (20200 seconds) post the GRB trigger. It faded down to $R = 21.3 \pm 0.2$, indicating a decay slope of ~ 1.2 in the time interval since $t > 5500$ seconds. Due to the orbit constraint of Swift satellite, there is no XRT observation in the time interval [2200, 5500] seconds when the optical lightcurve features as a plateau. The fading behavior of the X-rays in the time interval [5500, 7700] seconds are similar to the optical afterglow. At $t \sim 0.2342$ day, the detected X-rays are also consistent with the optical emission. These results suggest that the temporal behavior of both the optical and X-ray afterglow would be the same. We thus make temporal analysis on the well-sampled optical lightcurve only. Both optical lightcurves in the time intervals before and after 2200 seconds are well fit with a smooth broken power-law,

$$F = F_0 \left[\left(\frac{t}{t_b} \right)^{\omega_{\alpha_1}} + \left(\frac{t}{t_b} \right)^{\omega_{\alpha_2}} \right]^{-1/\omega} \quad (1)$$

Our best-fit parameters are summarized in Table. 2. We find that the decay slopes post the two breaks are unchanged, keeping as ~ 1.22 . The X-ray data at $\sim 4 \times 10^5$ is also consistent with the fit for optical data at the late epoch.

3.2 Data Confronting with Forward Shock Models

As shown above, the temporal features of the lightcurves in the optical and X-ray band are achromatic, and the decay slopes post the two breaks observed in the optical lightcurve are well consistent with the prediction of the forward shock models. In addition, the the ao-ax is consistent with the forward shock models (e.g. Urata et al. 2007). We find no spectral evolution cross the two breaks from the X-ray data. The derived β_X are 1.09 ± 0.15 and 1.03 ± 0.10 for the X-ray spectra accumulated in $t < 2200$ s and $t > 2200$ s, respectively. The β_X and temporal decay index in the normal decay segment post the early breaks are in good agreement with the closure relation of forward shock models in the spectral regime $\nu > \max(\nu_m, \nu_c)$, $\alpha = (3\beta_X - 1)/2 = 1.14 \pm 0.23$, where ν_m and ν_c are the typical and cooling frequencies of the synchrotron radiation. These results imply that the two shallow decay segments or plateaus in the optical lightcurves would be due to two epoches of energy injection from GRB central engine (e.g., Dai et al. 1998; Zhang & Meszaros et al. 2001; Liang et al. 2007).

3.3 Constraint on Burst Environment

Burst environment is critical to understand the burst nature. As shown above, at a very early epoch, the ν_c is below the optical bands. This may place constraints on the burst environment and microphysical parameters. Since the observed flux in the spectral regime $\nu > \nu_c$ is independent of the medium surrounding the bursts, we lost constraints of the

medium property with our observations. In principal, there are two types of medium surrounding the burst, i.e., wind medium and constant medium. If the medium surrounding the burst is wind medium, the burst would be confidently produced by collapse of a massive star. Therefore, our analysis below focus on case the constant medium only.

For a constant density medium, the typical synchrotron emission frequency, the cooling frequency and the peak spectral flux (Sari et al. 1998; coefficients taken from Yost et al. 2003; Zhang et al. 2007b) are:

$$\nu_m = 3.3 \times 10^{12} \text{ Hz} \left(\frac{p-2}{p-1} \right)^2 (1+z)^{1/2} \epsilon_{B,-2}^{1/2} \epsilon_{e,-1}^2 E_{K,52}^{1/2} t_d^{-3/2} \quad (2)$$

$$\nu_c = 6.3 \times 10^{15} \text{ Hz} (1+z)^{-1/2} (1+Y)^{-2} \epsilon_{B,-2}^{-3/2} E_{K,52}^{-1/2} n^{-1} t_d^{-1/2} \quad (3)$$

$$F_{\nu, \max} = 1.6 \text{ mJy} (1+z) D_{28}^{-2} \epsilon_{B,-2}^{1/2} E_{K,52} n^{1/2} \quad (4)$$

where νF_ν is the observed flux, D is the luminosity distance in units of 10^{28} cm, f_p is a function of p ($f_p \sim 1$ for $p = 2$), t_d is the observer's time in unit of days. The notation Q_n denotes 10^n in cgs units. Y is the Inverse Compton scattering parameter,

$$Y = [-1 + (1 + 4\eta_1 \eta_2 \epsilon_e / \epsilon_B)^{1/2}] / 2, \quad (5)$$

where $\eta_1 = \min[1, (\nu_c / \nu_m)^{(2-p)/2}] \sim 1$ for $p \sim 2.0$ (Sari & Esin 2001), and $\eta_2 \leq 1$ is a correction factor introduced by the Klein-Nishina correction. We take $\eta_2 = 1$ in our analysis.

$$\begin{aligned} \nu_R F_{\nu_R} &= F_{\nu, \max} \nu_c^{1/2} \nu_m^{(p-1)/2} \nu_R^{(2-p)/2} \\ &= 2.67 \times 10^{-11} f_p \text{ ergs s}^{-1} \text{ cm}^{-2} D_{28}^{-2} (1+z)^{(p+2)/4} \\ &\times (1+Y)^{-1} \epsilon_{B,-2}^{(p-2)/4} \epsilon_{e,-1}^{p-1} E_{K,52}^{(p+2)/4} t_d^{(2-3p)/4} \nu_R^{(2-p)/2} \end{aligned} \quad (6)$$

where

$$f_p = \left[7.45 \times 10^{-3} \left(\frac{p-2}{p-1} \right)^2 \right]^{(p-1)/2} \quad (7)$$

Since $p = 2\beta = 2.18 \pm 0.30$, we have $f = 6.04 \times 10^{-3}$. One can derive E_K at any time t_d as (Zhang et al. 2007b):

$$\begin{aligned} E_{K,52} &= \left[\frac{\nu_R F_{\nu_R}}{1.61 \times 10^{-13} \text{ ergs s}^{-1} \text{ cm}^{-2}} \right]^{4/(p+2)} \\ &\times D_{28}^{8/(p+2)} (1+z)^{-1} t_d^{(3p-2)/(p+2)} \\ &\times (1+Y)^{4/(p+2)} \epsilon_{B,-2}^{(2-p)/(p+2)} \\ &\times \epsilon_{e,-1}^{4(1-p)/(p+2)} \nu_R^{2(p-2)/(p+2)}. \end{aligned} \quad (8)$$

The analysis above is valid for $p > 2$. From the X-ray data, we find the p is slightly larger than 2. In order to make rough estimate, we take $p \sim 2$ to simplify Eq. 8 as

$$E_{k,52} = \frac{\nu_R F_{\nu_R}}{1.61 \times 10^{-13} \text{ ergs s}^{-1} \text{ cm}^{-2}} \frac{t_d}{1+z} \epsilon_{e,-1} (1+Y) D_{L,28}^2 \quad (9)$$

The ν_c is given by

$$\begin{aligned} \nu_c &= 6.3 \times 10^{15} \text{ Hz} \left(\frac{\nu_R F_{\nu_R}}{1.61 \times 10^{-13} \text{ ergs s}^{-1} \text{ cm}^{-2}} \right)^{-1/2} \\ &\times (1+Y)^{-5/2} \epsilon_{B,-2}^{-3/2} \epsilon_{e,-1}^{-1} n^{-1} t_d^{-1} D_{28}^{-1}. \end{aligned} \quad (10)$$

At $t \sim 100$ seconds, $\nu_R F_{\nu_R} = 4.42 \times 10^{-12} \text{ erg cm}^{-2} \text{ s}^{-1}$.

We have

$$\nu_c = 1.57 \times 10^{17} \text{ Hz} (1 + Y)^{-5/2} \epsilon_{B,-2}^{-3/2} \epsilon_{e,-1}^{-1/2} n^{-1}. \quad (11)$$

The requirement of $\nu_R > \nu_c$ at $t \sim 100$ seconds gives

$$n > 354s(\epsilon_e, \epsilon_B), \quad (12)$$

where $s(\epsilon_e, \epsilon_B) = \epsilon_{B,-2}^{-3/2} \epsilon_{e,-1}^{-1/2} (1 + Y)^{-5/2}$. It is found that as ϵ_B increases, s dramatically decreases. Considering an extreme case of energy equipartition among radiating electrons, magnetic field and baryons, i.e., $\epsilon_e = 1/3$, $\epsilon_B = 1/3$, we get $n > 0.6 \text{ cm}^{-3}$, indicating the burst should happen in a medium environment similar to Type II GRBs.

4 DISCUSSION AND CONCLUSIONS

We have presented the early optical observations for GRB 090426 with TNT and LOAO. Our well-sampled optical afterglow lightcurve from ~ 90 seconds to $\sim 10^4$ seconds post the GRB trigger seems to exhibit two energy injection phases ended at ~ 230 seconds and ~ 7100 seconds, respectively. The temporal feature of the observed X-rays is consistent with the optical emission. We show that both the optical and X-ray afterglows are consistent with the forward shock models in the spectral regime $\nu > \max(\nu_m, \nu_c)$. Although the medium property is lost constraints with the observed X-ray and optical flux due to they are independent of the medium surrounding the bursts, the fact that ν_c is below the optical bands at a very early epoch suggests a medium density comparable to that observed in Type II GRBs, if the burst is in an inter-stellar medium.

GRB 090426 is of interest with its short duration ($T_{90} \sim 0.33$ seconds in the burst frame) and high redshift ($z = 2.609$). Its redshift significantly exceeds the previous spectroscopically confirmed high redshifts for short GRBs 070714B ($z = 0.904$) and 050521 ($z = 0.546$). Its host galaxy is a blue, luminous, and star-forming galaxy (Levesque et al. 2010), similar to the host galaxies of typical Type II GRBs. Both the spectrum-energy correlation in the prompt gamma-ray phase and the host galaxy feature of GRB 090426 also suggest that this event would be physically from the death of a massive star, but not from merger of compact stars as typical short duration GRBs. With the new classification method proposed by Lv et al. (2010), GRB 090426 is also well grouped into Type II GRBs, but GRBs 051221 and 070714B are of the Type I GRBs. We also noted that GRB 090426 has some similar properties with another Type II burst, GRB 040924, which was a short-duration (1.2-1.5 sec), soft spectrum (Huang et al. 2005) and a SN 1998bw-like supernova-associated burst (Soderberg et al. 2006; Wiersema et al. 2008). The early afterglows could be an independent probe for the nature of this event. Our results well favor the idea that the burst is a Type II event.

5 ACKNOWLEDGEMENT

This work made use of data supplied by the UK *Swift* Science Data Center at the University of Leicester. It is partially supported by the National Natural Science Foundation of China under grants No. 10673014, 10803008, 10873002, and the National Basic Research Program ("973" Program)

of China under Grant 2009CB824800. It is also partly supported by grants NSC 98-2112-M-008-003-MY3 (Y.U.). Besides, this work is also partially supported by NASA NNX09AT66G, NNX10AD48G, and NSF AST-0908362. E. W. L. acknowledges the support from Guangxi SHI-BAI-QIAN project (Grant 2007201), the program for 100 Young and Middle-aged Disciplinary Leaders in Guangxi Higher Education Institutions, and the research foundation of Guangxi University(M30520). MI and YS are supported by the Korea Science and Engineering Foundation (KOSEF) grant No. 2009-0063616, funded by the Korean government (MEST).

REFERENCES

- Adelman-McCarthy J. K., et al., 2008, ApJS, 175, 297
 Antonelli L. A., et al., 2009, A&A, 507, L45
 Barthelmy S. D., et al., 2005, Natur, 438, 994
 Belczynski K., Holz D. E., Fryer C. L., Berger E., Hartmann D. H., O'Shea B., 2010, ApJ, 708, 117
 Berger E., et al., 2005, ApJ, 634, 501
 Cummings J. R., et al., 2009, GCN, 9254, 1
 Dai Z. G., Lu T., 1998, A&A, 333, L87
 Eichler D., Livio M., Piran T., Schramm D. N., 1989, Natur, 340, 126
 Evans P. A., et al., 2009, MNRAS, 397, 1177
 Fox D. B., et al., 2005, Natur, 437, 845
 Fynbo J. P. U., et al., 2006, Natur, 444, 1047
 Gal-Yam A., et al., 2006, Natur, 444, 1053
 Gehrels N., et al., 2005, Natur, 437, 851
 Gehrels N., et al., 2006, Natur, 444, 1044
 Greiner J., et al., 2009, ApJ, 693, 1610
 Han W., et al., 2005, PASJ, 57, 821
 Huang K. Y., et al., 2005, ApJ, 628, L93
 Im M., Jeon Y., Lee I., Jeon Y.-B., Urata Y., 2009, GCN, 9276, 1
 Kouveliotou C., Meegan C. A., Fishman G. J., Bhat N. P., Briggs M. S., Koshut T. M., Paciesas W. S., Pendleton G. N., 1993, ApJ, 413, L101
 Levesque E., Chornock R., Kewley L., Bloom J. S., Prochaska J. X., Perley D. A., Cenko S. B., Modjaz M., 2009, GCN, 9264, 1
 Levesque E. M., et al., 2010, MNRAS, 401, 963
 Liang E.-W., Zhang B.-B., Zhang B., 2007, ApJ, 670, 565
 Liang E., Zhang B., 2005, ApJ, 633, 611
 Lin L., Liang E.-W., Zhang B.-B., Zhang S. N., 2008, AIPC, 1065, 39
 Lin L., Liang Enwei, Zhang Shuang Nan, 2009, arXiv, arXiv:0906.3057
 Lv H., Liang E., Zhang B., Zhang B., 2010, arXiv, arXiv:1001.0598
 McGlynn S., Foley S., McBreen S., Hanlon L., O'Connor R., Carrillo A. M., McBreen B., 2008, A&A, 486, 405
 Nakar E., 2007, PhR, 442, 166
 Narayan R., Paczynski B., Piran T., 1992, ApJ, 395, L83
 Norris J. P., Bonnell J. T., 2006, ApJ, 643, 266
 Paczynski B., 1998, ApJ, 494, L45
 Perley D. A., et al., 2009, ApJ, 696, 1871
 Piran T., 2004, RvMP, 76, 1143
 Rumyantsev V., Antonuk K., Pozanenko A., 2009, GCN, 9312, 1

- Sakamoto T., et al., 2009, ApJ, 693, 922
Salvaterra R., et al., 2009, Natur, 461, 1258
Sari R., Piran T., Narayan R., 1998, ApJ, 497, L17
Sari R., Esin A. A., 2001, ApJ, 548, 787
Sato G., et al., 2009, GCN, 9263, 1
Schlegel D. J., Finkbeiner D. P., Davis M., 1998, ApJ, 500, 525
Soderberg A. M., et al., 2006, ApJ, 636, 391
Tanvir N. R., et al., 2009, Natur, 461, 1254
Thoene C. C., et al., 2009, GCN, 9269, 1
Urata Y., et al., 2003, ApJ, 595, L21
Urata Y., et al., 2005, NCimC, 28, 775
Urata Y., et al., 2007, ApJ, 668, L95
Virgili F. J., Zhang B., O'Brien P., Troja E., 2009, arXiv:0909.1850
Villasenor J. S., et al., 2005, Natur, 437, 855
Wiersema K., et al., 2008, A&A, 481, 319
Woosley S. E., 1993, ApJ, 405, 273
Woosley S. E., Bloom J. S., 2006, ARA&A, 44, 507
Xin L. P., Zheng W. K., Qiu Y. L., Wei J. Y., Wang J., Deng J. S., Urata Y., Hu J. Y., 2009, GCN, 9255, 1
Xin L. P., et al., 2010, MNRAS, 401, 2005
Yost S. A., Harrison F. A., Sari R., Frail D. A., 2003, ApJ, 597, 459
Zhang B., Mészáros P., 2001, ApJ, 552, L35
Zhang B., Mészáros P., 2004, IJMPA, 19, 2385
Zhang B., Fan Y. Z., Dyks J., Kobayashi S., Mészáros P., Burrows D. N., Nousek J. A., Gehrels N., 2006, ApJ, 642, 354
Zhang B., Zhang B.-B., Liang E.-W., Gehrels N., Burrows D. N., Mészáros P., 2007a, ApJ, 655, L25
Zhang B., et al., 2007b, ApJ, 655, 989
Zhang B., et al., 2009, ApJ, 703, 1696
Zheng W.-K., et al., 2008, ChJAA, 8, 693